

Recombination mechanisms in crystalline silicon: bulk and surface contributions

Enrichetta Susi

Istituto LAMEL-CNR, via Gobetti 101, Bologna, Italy

ABSTRACT. In the present paper the most interesting results of a work on the influence of some processes used in the fabrication of microstructures on the bulk and surface electrical activity of the Si substrate are reported. In these studies the minority carrier lifetime and the surface recombination velocity were used as sensors of the Si electrical activity changes. Other electrical (DLTS, C - V and I - V characteristics, EBIC) and structural (X-ray double crystal diffractometry, IR spectroscopy) techniques were used to gather information about the nature and concentration of the defects induced by processing.

Two processes have been investigated: Rapid Thermal Annealing treatments (RTA), and Reactive Ion Etching (RIE): neither of them have a large influence on the minority carrier diffusion length when the substrate is an high quality Si wafer of the last production. On the contrary, the surface recombination velocity is largely influenced by both processes. The rearrangement of the surface structure and the formation and growth of hillocks is proposed as the more important mechanism responsible of the observed changes in the surface electrical activity.

1. INTRODUCTION

Bulk minority carrier recombination lifetime is one the most studied parameters since the birth of the semiconductor physics. In the past most studies were prompted by its importance in the solar cell performance. Today minority carrier lifetime is knowing a renewed favour in the Si IC community, because it is one of the few parameters sensitive to the very low defect densities consistent with the present IC's technology [1, 2]. Its use to control the defects induced by the processing steps is now widespread.

In spite of the huge mass of experimental work performed on this topic, many questions are still unresolved, owing to the limits of the techniques used to measure the minority carrier lifetime, to its high but not selective sensitivity to the defect presence, and to the influence of many other parameters. In the following the most important defects controlling the lifetime behavior are discussed and what is known about the interactions between defects occurring during the processing is outlined.

Like in the case of lifetime, the most significant contributions to the Si surface recombination velocity measurement were made in the seventies by the solar cell technology specialists. In the last years the effort to improve the lifetime measurements has induced a new attention on surface electrical properties. Moreover, as the feature sizes of the devices shrink, the role of surface is becoming critical for the IC's technology, so that many research groups are now working on the surface structural and electrical properties. The most interesting results were up to now obtained by the structural measurements.

The electrical characterization is less developed: most part of the available data were obtained from multiple parameter fitting of the behavior of diodes, MOS capacitors or solar cells, while only few refer to the bare

Si surface so much less is known about the recombination mechanisms at the surface and about the influence of defects on the surface electrical behavior.

1.1. Electrically active defects in Si. The most important defects having a direct or indirect influence on the electrical characteristics of silicon are:

Extrinsic defects. 1. Oxygen related defects: thermal donors and new thermal donors, oxygen clusters and precipitates,

2. metal impurities and their complexes: fast diffusing metal atoms, acceptor-metal complexes, precipitates,

3. extended defects: dislocations and slip lines, stacking faults.

Intrinsic defects. Si self interstitial and vacancies, and their agglomerates

Oxygen is incorporated in CZ silicon as atom during the growth process at concentrations higher than the solubility limit. The system is therefore thermodynamically out of equilibrium. After the growth any process involving thermal treatments will induce various stage of precipitation and phase segregation of supersaturated oxygen, giving rise to different defects, both neutral and electrically active. Their influence on lifetime has been extensively investigated for their role in impurity gettering during device processing [3].

The thermal donors are oxygen clusters with double donor electrical activity, having mean activation energy of respectively 0.07 and 0.15 eV for the ionization of the neutral and single positive state charges. They form upon heating at $300 > T < 500$ °C, and are removed at 650 °C. The so called "new thermal donors" form near 700 °C and are connected to the presence of carbon impurities. These defects have been extensively studied for many years, without attaining a clear picture of their structure. Their effect on recombination of minority carriers is likely to be weak [4].

Neutral oxygen clusters are supposed to be present in the as grown Si as a consequence of the cooling after the crystal growth and/or thermal donor stabilization preanneal. They don't have any influence on the electrical behavior of the material but are involved in the complex nucleation process of oxygen precipitates [5] and in the gettering activity of oxygen.

The formation of oxide precipitates during thermal processing is known to be one of the main factors determining the carrier recombination [6]. The formation of these precipitates is accompanied by the nucleation of extended lattice defects which attract the impurities present in the wafer and act as efficient recombination centers. Their influence on lifetime has been extensively investigated for their role in impurity gettering (the so called internal gettering) now routinely used in the device processing. Many aspects of the interactions between oxygen precipitates and the other defects present in the Si matrix are still a matter of conjectures.

Fast diffusing metal impurities, in particular transition metals like Fe, Ni and Cu have an essential role in degrading minority carrier lifetime. They are present in the as grown material or are introduced by contamination during the handling and processing of the wafers in condition of high supersaturation due to the strong dependence of the solubility on temperature. The control of metal contamination during processing is in fact one of the main problems of the today technology [7]. The transition metals high diffusion rate combined with the high supersaturation leads to exceptionally favourable conditions for the nucleation of precipitates, enhanced by the good fit of the coherent silicide phases to the silicon lattice. So during the cooling following the heat treatments the dissolved metals can precipitate as silicide in the Si lattice. These precipitates act as recombination centers and reduce lifetime. The reduction is controlled by the density of the precipitates and not by their chemical nature [8]. In fact the recombination takes place at the boundary between the foreign phase and the host Si lattice, and is almost independent of the chemical nature of the precipitate.

Transition metals can diffuse at the surface, where they form precipitates. These surface defects have been studied mainly as "haze" by light scattering at the etch pits on polished wafers; their effect on surface electrical properties is poorly known. Ni is known to precipitate preferentially at the surface, so the decrease of lifetime observed in p-type Ni contaminated Si wafers has to be attributed at these surface defects. No data are available on the influence on surface recombination velocity. For fast cooling rates the metals, in particular Fe, can remain dissolved. Very low concentrations of dissolved metals strongly reduce lifetime. The chemical nature of the dissolved metals and the dopant type and oxygen content of the Si substrate are very important in determining the effect on lifetime. For instance:

(1) Fe reduces strongly the lifetime in p-type Si and much less in n-type Si, and in FZ more than in CZ crystals [9],

(2) Cu reduces lifetime in n-type Si but not in p-type Si [10].

The reason of these dependences is to be found in the influence of capture cross sections for the minority carrier, that may be different for electrons and holes and may vary by many orders of magnitude for different metals. The difference between FZ and CZ crystals can be ascribed to the gettering activity of oxygen.

The transition metals tend to diffuse toward extended defects and to increase their electrical activity by decorating them; they can enhance the formation of extended defects.

Dissolved metals can form pairs and compounds with other impurities and with dopant atoms. The transition metal interstitial donors form neutral pairs with acceptor (D^+A^-), bound by the Coulomb interaction, of which the most familiar is the Fe_iB_s pair. These pairs are bistable or metastable: the ground state of the neutral pair is at nearest neighbour separation, but there are many metastable configurations associated with the discrete more distant lattice separation. The conversion from one to another configuration depends on temperature, but can be induced by illumination, biasing and so on. The Fe_iB_s pairs form two deep energy levels in the Si band gap, so they can influence lifetime differently from interstitial Fe, due to the different capture cross sections.

As grown Si wafers are free from extended defects. Extended defects like dislocations, slip lines, dislocation loops and stacking faults can be produced by the treatments that induce mechanical stresses, (like an high temperature anneal with an uneven temperature distribution) or phase transitions (like the precipitation of oxygen or other impurities). The existence of an intrinsic recombination activity of extended defects is still a controversial question. It is likely that their influence on lifetime is due mainly to the decoration with fast diffusing impurities [11].

The intrinsic defects are much less known than the extrinsic ones. Si self interstitials and vacancy are present at high concentrations during the growth of the crystals and are frozen in the crystal bulk during cooling. Agglomeration of such defects are thought to be the origin of the microdefects, like swirls and D defects, inhomogeneously distributed small defect clusters. The swirls can act as heterogeneous nucleation centers for oxygen precipitation, and are thought to deteriorate lifetime. Other defects likely to be related to vacancy clusters are surface flaws detected at the surface of polished Si wafers and called Crystal Originated Particles (COP) [12].

1.2. Recombination lifetime and surface recombination velocity as sensors of the process induced damage: problems and results. Many of the results on the recombination activity of defects above reported were obtained after special sample preparations allowing to single out the desired parameter. For instance, the effect of dissolved transition metals on lifetime has been

measured introducing carefully controlled amounts of a particular metal in the Si wafer. In the real life, that is during the handling and processing of wafers, many different defects, usually unevenly distributed, are simultaneously present, and undergo multiple and complex interactions. So no single technique allows a thorough understanding of the process; moreover very few are the electrical measurement techniques suitable to the purpose.

The minority carrier lifetime has a high sensitivity, and can monitor the effect of a single processing step on the defect recombination activity: due to its low selectivity, however, it is not suitable for the identification of the involved defects. So the study of the changes in Si electrical properties after processing needs the use of many electrical and structural techniques, to detect and characterize the defects.

The surface recombination velocity quantifies the recombination at a semiconductor surface, and is therefore very sensitive to small changes in the surface recombination activity. To measure it is however a difficult task. A series of limitations are imposed on most of the techniques currently employed [13], and caution must be used in the interpretation of the experimental data, because often the experimental conditions don't fulfill the requirements of the model. So little is known about the mechanisms controlling the recombination activity at the surface and the role of the surface structure and of the defect presence.

The author has carried a systematic study of the effects on the electrical behavior of Si wafers of thermal treatments by Rapid Thermal Annealing (RTA): in the RTA a wafer is brought to a high temperature for a very short time: the energy source is a system of incoherent radiation lamps. The process is widely used in the ULSI technology due to the possibility to avoid the dopant diffusion and to reduce the thermal budget. The minority carrier lifetime was used as a sensor of the recombination activity changes, while other electrical (DLTS, resistivity and Hall effect, C-V and I-V characteristics) and structural (X-ray double crystal diffractometry, IR spectroscopy) techniques were used for the detection and the identification of the process induced defects [14, 15].

It was so possible to understand the nature and electrical properties of the defects induced by the lamp RTA in virgin Si, and their interactions with dopant and residual impurities (oxygen, carbon, metals). We observed a reduction of the minority carrier lifetime after RTA for temperatures higher than 750 °C. The defect responsible for this diminution was identified by DLTS as a donor with an energy level at $E_V + 0.29$ eV and an electron capture cross section of 1.1×10^{-15} cm², that can be identified as interstitial Cr associated with substitutional B. The source of this defect was proved to be the activation of pre-existing precipitates or other aggregates in an electrically inactive state. A gettering role of oxygen clusters was observed at temperatures around 750 °C [16].

During this work an unexpected large increase of the surface recombination velocity after RTA was detected. This increase depended on temperature and on time. From the C-V and DLTS measurement the introduction of donor levels at the surface was detected. A contribution of oxygen was supposed, due to the difference in the intensity of the effect between CZ and FZ wafers. In p-type Si the effect was stronger on the bulk parameters (lifetime and resistivity) and weaker on the surface parameters (surface recombination velocity and surface state density). The opposite held for n-type Si. A systematic study in which the monitoring of the surface recombination velocity was used as a tool to detect the process induced damage with an even larger sensitivity than minority carrier lifetime was then set off.

Our work in this field has been characterized by the effort to improve the reliability of the surface recombination velocity measurements and to correlate them with the data on surface damage obtained by other structural and electrical methods. To improve the reliability of the surface recombination velocity data we used three independent methods; the Photoelectromagnetic (PEM) effect, which allows the direct determination of the surface recombination velocity from the dependence on the incident light intensity of the photoinduced magnetic effect, a combination of SPV (surface photovoltage) and Photocurrent (λ -PC) and the Electron Beam Induced Current (EBIC) mode of the Scanning Electron Microscope. The last technique allows a direct imaging of the recombining defects and a calculation of the local surface recombination velocity.

In addition to RTA the damage induced by the Reactive Ion Etching was studied. The anisotropic selective ion etching, now widely used in the fabrication of micro structures, is known to induce damage in the materials being etched. Three types of dry etching damages have been identified [17]: residue or R-layer, that is films of foreign material deriving from the chemical reactions at the surface, a permeated or P-layer, basically Si permeated by etching species and impurities, and a bonding damaged Si layer (D-layer) deriving from the ion bombardment and radiation exposure. In the last times evidence has been found that dry etching can roughen the Si surface [18]. Two different etching chemistries were studied, namely the dry etch of SiO₂ by a CHF₃/Ar plasma, where the most important damage is the deposition of a fluorocarbon R-layer and the dry etch by SiCl₄ of poly-Si films, where the residue effects are negligible, while the P and D layer are present [19]. Wet etched control samples were used to distinguish the defects induced by the processing in itself from the RIE induced defects. The influence of rf power was studied.

The results obtained on the damage induced by the dry etch of SiO₂ by a CHF₃/Ar plasma have been published elsewhere [20, 21]. A large increase of the surface recombination velocity in the low rf power etched samples was observed: the only detected damage was due to the presence of a fluorocarbon residue layer, to which the increase in the surface electrical activity was

ascribed.

Here we report the results obtained in the study of the Si substrate after a SiCl_4 etching of the poly-Si film:

2. MATERIALS AND METHODS

2.1. Samples And Processing

A. Rapid Thermal Annealing. 200 mm (100)-oriented wafers of B-doped CZ Si, resistivity 12 ohm·cm were used. To allow the comparison between samples with the same thermal history and similar initial defects content all the measurements were performed on the same samples or in samples from adjacent zones.

The anneals have been performed at 750 °C and 1000 °C for 60 sec in Ar in a commercial AG Associates Heat Pulse lamp system.

B. Reactive Ion Etching. Four inch (100)-oriented wafers of phosphorus doped CZ silicon, resistivity 1 ohm·cm were used. A 5500 Å thick polysilicon film was grown by Low Pressure Chemical Vapor Deposition at 607 °C for 65 min at a pressure of 170 mTorr P-doped by diffusion from a POCl_3 glass at 920 °C, and oxidized at 950 °C for 10 min. In a group of samples before the poly deposition a 550 Å gate oxide was grown by wet oxidation at 900 °C. The poly-Si layer was dry etched by a SiCl_4 plasma. Two different rf powers (processes A, B) were used in order to study the effect of rf bias on the induced damage. The etch times were calibrated to remove all the polysilicon, without any appreciable Si overetching. Reference wafers, subjected to the same processing steps as the dry etched samples, were etched by a conventional chemical wet etch (process C), in order to separate the effect of the dry etch from the influence of the processing needed for the preparation of the test structures. The detailed process conditions are listed in Table 1. The samples where a gate oxide was interposed between the poly-Si film and the Si substrate (called A1, B1, C1) were processed in the same way as the corresponding A, B, C plus a wet etch to remove the gate oxide at the end of the processing. For the sake of brevity reference samples will henceforth be called respectively C and C1, the samples etched at low rf power B and B1, and the samples etched at high rf power A, and A1.

The detailed etching conditions are listed in Table 1.

2.2. Measurements. The following electrical parameters were monitored:

- Resistivity by the standard four point technique.
- Minority carrier diffusion lengths and surface recombination velocity by three independent methods, a combination of SPV (surface photovoltage) and Photocurrent, a combination of the PhotoElectromagnetic effect (PEM) and steady state PhotoConductivity (PC), and the Electron Beam Induced Current (EBIC).

The standard analysis of these methods relies on several simplifying assumptions suitable for diffusion lengths short compared with the wafer thickness. The 200 mm wafers used for RTA experiments have diffusion lengths larger than the wafer thickness, so an extension of the analysis has been necessary. For PEM-PC minority carrier lifetime and surface recombination velocity were obtained by measuring the two effects at different wavelengths and fitting the dependence of their ratio on the absorption constant using the equation of Gärtner [22].

For SPV we used the enhanced method proposed by Lagowski [23], to obtain the minority carrier diffusion length. The surface recombination velocity was obtained by the wavelength dependence of the photocurrent. The experimental set-up is the same as the SPV method, the fundamental difference is the wavelength range employed; here strongly absorbed light impinges the sample surface and generates charge carriers which recombine at the surface. By increasing the wavelength the absorption coefficient decreases and the carriers are generated in the bulk of the semiconductor. From the variation of the photocurrent as a function of the absorption coefficient the surface recombination velocity can be obtained, using a theoretical model proposed by De Vore [24]. In this procedure the only fitting parameters are the surface recombination velocity and a normalization factor, as the minority carrier diffusion length is known by the previous techniques.

In the case of the EBIC technique such an adjustment was not possible, so this technique has not been used in the RTA experiments.

- Energy levels, concentration and distribution of traps by the Deep Level Transient Spectroscopy (DLTS). DLTS spectra from 40 K to 320 K were recorded using a

Table 1. Process conditions used in the etching of the polysilicon film.

PROCESS	A	B	C	A1	B1	C1
Chemistry:	SiCl_4	SiCl_4	Buffered ($7\text{NH}_4\text{F} : 1\text{HF}$) + poly etch $1\text{HF} : 50$ HNO_3	A+ buffered HF	B+ buffered HF	C+ buffered HF
rf power:	0.89 W/cm ² 13 min	0.89 W/cm ² 8 min			0.22 W/cm ² 9 min	
Pressure:	36 mtorr	36 mtorr				
Gas flow rate:	16.5 sccm	16.5 sccm				

Polaron DL4600 with a helium cryostat. The trap profiles were obtained by the Double DLTS (DDLTS) technique.

- Quality of the Schottky barriers and dopant concentration by the Capacitance-Voltage (C-V) and Current-Voltage (I-V) techniques. A special attention was paid to the preparation of the Schottky diodes.

To study the influence of RTA on the surface properties we needed to avoid the usual etching before the metal deposition, keeping acceptable the diode quality. The best results were obtained by washing the samples in 2-butanone before the evaporation through a metal mask of the 3.14 mm² Al dot. For the back contact a 70% In -30% Hg alloy was used. The samples were mounted on a purposely made holder, with a spring controlled point contact, so that the same diode could be used in different measurements (DLTS, EBIC, SPV, photocurrent) without damaging it.

The RIE etched wafers were divided in 4 parts: the first two were used for the C-V and I-V characteristics and DLTS spectra the 0.45 mm² Au Schottky diodes were evaporated through a metal mask on the as processed surface. Electroless Ni ohmic contact were deposited onto the back side. The other two quarters of the as treated wafers were used for the PEM measurements, and for the EBIC and SPV observations. In the sample to be studied by EBIC and SPV the Schottky diodes were prepared in the same way as the diodes used for the C-V and DLTS measurements, but for the area (5 mm²) and the thickness (200 Å) of the Au dot.

3. RESULTS AND DISCUSSION

The distribution in the Si wafers of the most important electrical parameters (resistivity, minority carrier diffusion length, surface recombination velocity, electrically active defects energy and concentrations) was accurately tested before the processing.

In the 200 mm p-type wafers used for the RTA anneals diffusion length around 750 μ , and surface recombination velocity values in the range 1000-10000 cm/s were measured. Variations lower than 9% in diffusion length were observed between samples taken at different zones of the wafer; the variations in surface recombination velocity were of the order of 40%. The presence of a deep level with an activation energy around 450 meV was detected (Figure 1). The trap has a concentration at the surface varying between 1.4 and 1.7 $\times 10^{14}$ (cm⁻³). Correspondingly an anomalous behavior (deviation from the linearity in the region around $V = 0$) of the C-V characteristics is observed. Such deviations from linearity are well known as due to the presence of deep states [25]: in p-type Si it is usually attributed to the passivation of B by hydrogen, which has been found to be released at the Si surface by all the standard cleaning and etching treatments [26]. The trap observed by DLTS could be connected to this passivation process.

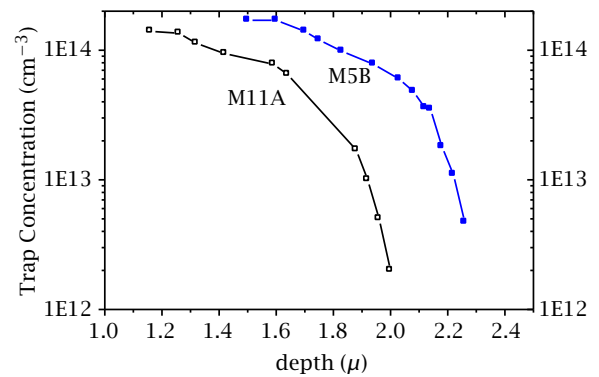


Figure 1. Profiles of the trap detected in the virgin wafer: the profiles were measured in different positions.

In the 100 mm n-type Si wafers used for the RIE treatments a distribution of diffusion lengths in the range 134-253 μ , with a mean value of 188 μ and of surface recombination velocities in the range 1-3 $\times 10^4$ cm/sec was detected. This variability had to be accounted for in the evaluation of the process induced changes in the two parameters. In fact the inhomogeneity observed in the starting wafers was still present in the dry etched as well as in the reference samples, so only variations larger than 35% for lifetime and 50% for surface recombination velocity were considered meaningful.

A. RTA. In Table 2 the variations in the diffusion length and surface recombination velocity after RTA at 750 °C and 1000 °C with respect to the values before the annealing are reported. The measurement of the diffusion length values by SPV after the RTA at 750 °C was difficult due to the presence of a strong photovoltaic effect. So only the PEM values are reported. The surface recombination velocity measurements with the photo current method were obtained using the PEM values for the diffusion length.

Table 2. Variations of minority carrier lifetime and surface recombination velocity in the RTA annealed samples with respect to the as received wafer obtained by the different measurement methods.

Thermal treatment	$\left[\frac{\Delta S}{S}\right]_{PEM}$	$\left[\frac{\Delta L}{L}\right]_{PEM}$	$\left[\frac{\Delta S}{S}\right]_{Photoc.}$	$\left[\frac{\Delta L}{L}\right]_{SPV}$
750 °C	+17	-0.10	+10	-
60 sec				
1000 °C	+1.9	-0.67	+1.3	-0.65
60 sec				

In Table 3 and 4 the DLTS peaks observed in the samples annealed at 750 °C and 1000 °C are reported. In the 750 °C annealed samples 3 traps were detected: all the three had profiles rapidly decaying in the first micron under the surface. Their distribution along the sample surface was uneven; only the trap 2 was detected in all the measured diodes.

Table 3. Mean values of the Arrhenius plot activation energies, and temperatures of the DLTS peaks in 750 °C annealed samples: in the last row the maximum and minimum detected trap concentration are reported.

Trap	1	2	3
E_A (eV)	0.6	0.4	0.26
T(100/s)	320 K	250 K	145 K
N_T (cm ⁻³)	1.3×10^{14}	1.1×10^{14}	5×10^{12}
	—	8×10^{11}	—

Table 4. Mean values of the Arrhenius plot activation energies, and temperatures of the DLTS peaks in 1000 °C annealed samples in: the last row the maximum and minimum trap concentration at the surface are reported.

Trap	1	2	3	4
E_A (eV)	0.6	0.4	0.4	0.2
T(100/s)	320 K	250 K	215 K	165 K
N_T (cm ⁻³)	2.4×10^{14} – 5×10^{11}	1×10^{12}	5×10^{12}	1.3×10^{14} – 2×10^{12}

In Figure 2 the profiles of the traps in a diode where they were all present in a sufficiently high concentration is reported.

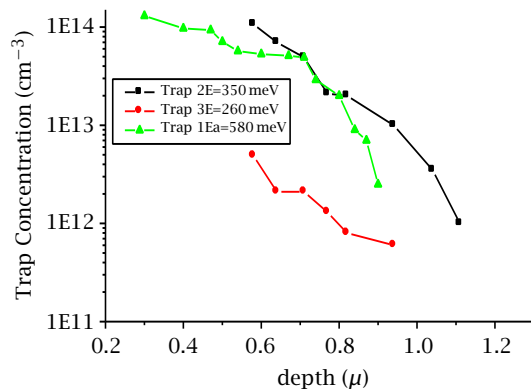


Figure 2. Profiles of the traps observed after RTA at 750 °C

A study of the same diodes by EBIC has allowed to detect an uneven distribution of electrically active extended defects. In Figure 3 a zone with many defects around 1 μ in dimensions are reported: in other diodes no defects were detected.

In the 1000 °C annealed samples only the traps 1 and 4 are present in all the measured diodes. Traps 1 and 2 correspond to the traps 1 and 2 observed in the 750 °C samples, but the trap 1 has a higher and the trap 2 a lower concentration. Traps 3 and 4 are observed only in the 1000 °C annealed samples. The profile of the traps 1, 2, 4 are reported in Figure 4 trap 1 has a profile similar to the profile observed in the 750 °C samples: trap 2 and 4 have a smooth profile. EBIC observation of the surface of the 1000 °C samples (Figure 5) detected a more uniform distribution of large extended defects (around 100 μ) at concentrations lower than the

defects observed in the defective zones of the samples annealed at 750 °C.



Figure 3. Defects observed in 750 °C annealed samples.

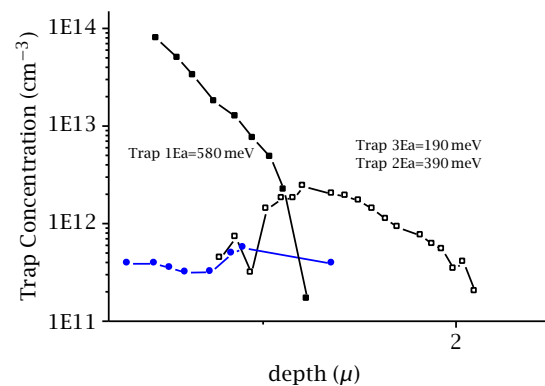


Figure 4. Profiles of the traps observed after RTA at 1000 °C

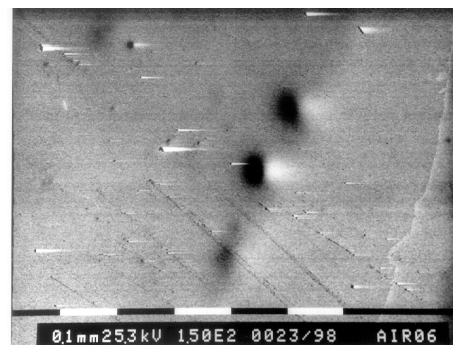


Figure 5. Defects observed in 1000 °C annealed samples.

In summary: The anneal at 750 °C for 60 sec produces a very little diminution of bulk minority carrier lifetime and a strong increase of surface recombination velocity. An inhomogeneous distribution of electrically active extended defects is present at the surface. Deep levels are present in a thin zone under the surface, and they cannot have a large influence on minority carrier bulk recombination.

The anneal at 1000 °C for 60 sec produces a noticeable (around 65%) diminution of lifetime and a less pronounced increase of surface recombination velocity. The defects observed by EBIC are more homogeneously distributed, larger and lower in number than the de-

fects observed in the 750 °C samples. Deep levels are detected at an higher depth, so that we can suppose a correlation between them and the observed reduction in the minority carrier diffusion length, obviously in the limits of the possibility of such a correlation between the results of a majority carrier technique, like DLTS in Schottky diodes, and a minority carrier parameter.

The surface recombination velocity has an increase much lower than in the 750 °C annealed samples.

Comparing these results with the results obtained in our previous work [26] on “old” (produced in 1985) 75 mm and “new” (produced in 1994) 100 mm wafers, we observe that the behavior of the bulk and surface parameters in the 200 mm wafers is similar to the behavior of the “new” 100 mm wafers: low effect of the 750 °C anneals on bulk lifetime, increase of surface recombination velocity larger in the 750 °C than in the 1000 °C annealed samples. Some important differences can however be outlined:

(1) At 750 °C the “recovery” effect previously observed at 60 sec is no more present,

(2) At 1000 °C the decrease in lifetime is lower (65% instead of 90%).

(3) The traps detected by DLTS are lower in number (4 instead of 7); the trap 3 (750 °C) and the traps 3 and 4 (1000 °C) of the present study are comparable with the traps H₂, H₃ and H₄ reported in [26]; the traps 1 and 2 were not detected in the sample used for the previous work.

(4) The surface concentrations of the traps of the present study are higher with respect to the concentrations reported in [26]: this can be due to the fact that in the previous studies we wet etched in the usual way the surface before the deposition of the Schottky contacts, etching away the first most damaged surface layer.

We can so conclude that the continuous reduction in harmful impurities content of the Si wafers is decisive in reducing the lifetime degradation for the high temperature anneals. Moreover, a reduction of 67% with respect to diffusion lengths of the order of 0.8 mm means diffusion lengths after the anneal around 0.5 mm with respect to the diffusion lengths around 0.08 mm of the 10 mm wafers. This result confirm our thesis that the mechanism responsible for the liferime reduction is the activation of the pre-existing impurities.

As for the surface modification, the present surface recombination velocity, DLTS and EBIC data confirm the existence of a surface damage. This damage is not influenced by the improvement in wafer quality. The ambient gas during the anneal doesn't have a direct influence: in the present work we used an Ar ambient instead of the N₂ ambient of the previous one, but the surface behavior did not change.

A question to explain is the higher increase of the surface recombination velocity in the samples annealed at a lower temperature. A role of the surface roughness due to local oxidation and/or etching connected to the presence of residual humidity in the anneal chamber [27] is the most likely explanation of the experimental data.

B. Reactive Ion Etching. A comparison of the diffusion length and surface recombination velocity average changes in the dry etched wafers with respect to the reference samples obtained by the three measurement methods is presented in Table 5. A fairly good agreement (taking into account the above reported uneven distribution of both parameters in the starting wafer) is observed for the diffusion length and surface recombination velocity values between the PEM and EBIC results: the data for surface recombination velocity obtained by the λ -PC method are much lower than the values obtained by the two other methods. The absolute values too of this parameter obtained by the λ -PC method are much lower than the values obtained by the two other methods. The reason of such a discrepancy can be the presence in all the samples of a surface barrier, revealed by the strong photovoltaic effect observed under illumination. In fact it is known that in the presence of a barrier the λ -PC method underestimates the surface recombination velocity, while the other two methods are not influenced. In fact when no barrier was present, like in the RTA annealed samples, the agreement between the PEM and the λ -PC surface recombination velocity data was very good.

No variations in the bulk minority carrier diffusion length is observed in the dry etched samples. An increase of the surface recombination velocity after the processes A, B and A1 is detected: the most remarkable increase, however, is observed after the process B (dry etching at a low rf power).

Table 5. Variations of the minority carrier diffusion length $L_{dry-Lwet}/L_{wet}$ and of the surface recombination velocity $S_{dry-Swet}/S_{wet}$ of the dry etched samples with respect to the wet etched ones for the three measurement methods:

Process	PEM		EBIC		SPV	λ -PC
	$L_{dry-Lwet}/L_{wet}$	$S_{dry-Swet}/S_{wet}$	$L_{dry-Lwet}/L_{wet}$	$S_{dry-Swet}/S_{wet}$	$L_{dry-Lwet}/L_{wet}$	$S_{dry-Swet}/S_{wet}$
A	-0.3	+3	+0.1	+1	-0.4	-0.6
B	-0.1	+19	+2	+8	-0.4	-0.1
A1	-0.1	+3	-0.6	+5	+1	-0.2
B1	+1	+0.1	+1	-0.1	-	-0.6

This behavior of the surface recombination velocity is somehow puzzling. In fact the data on the damage obtained by the C-V and I-V characteristics and from DLTS give evidence of a higher damage in the A and A1 samples with respect to the B and B1. In Table 6 the most important parameters obtained by the C-V and I-V characteristics of all the processed samples are reported. In the A and A1 samples a reduction of the barrier height and an increase of the leakage current with respect to the reference samples is observed. These two data are indicative of the presence respectively of a bonding damage and of a permeating layer. The B samples have a barrier height as expected and a leakage current higher than the reference samples, but lower than the A samples.

The DLTS data confirm this damage distribution. In Table 7 and 8 the traps detected in all the samples and their maximum concentration at the surface are reported. Three traps, E3, E4 and E7 are present only in the dry etched samples E5 and E6 are: present also in the reference samples, and are likely due to the deposition, doping and oxidation of the poly-Si film. The traps E1 and E2 are present only in the samples where the gate oxide was interposed between the Si substrate and the poly-Si film. The dry etching induced traps have higher concentrations in the samples A and B, while the process induced traps have higher concentrations in the samples A1, B1, C1. All the traps have profiles rapidly decaying in the first micron under the surface (Figure 6), so they don't have an influence on the bulk

minority carrier lifetime.

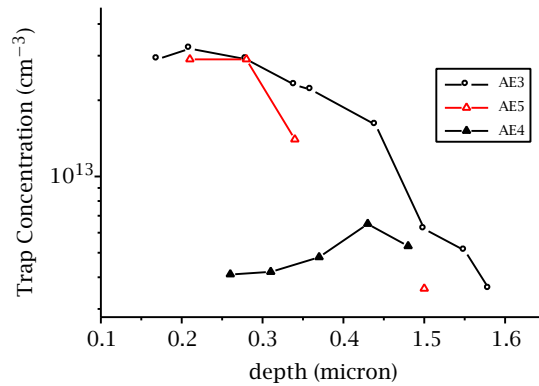


Figure 6. Profiles of the traps E3, E4, E5 in a A sample.

The slight increase of the surface recombination velocity in the A and A1 samples can be ascribed to higher bonding damage and contamination, but the large increase of the same parameter in the samples B is not explained by the damage data. On the other hand, as expected for the SiCl_4 chemistry, from the C-V and I-V data the presence of a R-layer (responsible of the surface recombination velocity increase in the samples etched in CHF_3/Ar) in the A and B samples can be excluded.

A key to an explanation of the data can be found in the images of the surfaces of samples A and B obtained by Atomic Force Microscopy (AFM) shown in Figure 7.

Table 6. Capacitance, barrier height, leakage current, ideality factor and slope resistance at high forward current of the Schottky diodes evaporated on the surface of the as processed samples.

Process	A	B	C	A1	B1	C1
$\phi(\text{V})$ from C-V	0.54	0.74	0.70	0.56	0.72	1.1
$J(-3\text{V})$ ($\mu\text{A cm}^{-3}$)	400	66	8	28	53	4
n	1.3	1.1	1.05	2.6	3	3
R_s (ohms)	25	25	43	5×10^4	3×10^4	5×10^5

Table 7. Arrhenius plot activation energies and peak temperatures of the traps observed in the A, B, C and A1, B1 and C1 samples.

Level	E1	E2	E3	E4	E5	E6	E7
E_a (meV)	560	410	380	380	330	310	200
T (100/s)	320K	290K	250K	230K	200K	176K	130K

Table 8. Distribution and concentration of the Table 7 levels after the different processes: the highest values are reported.

Process	E1	E2	E3	E4	E5	E6	E7
A	no	no	3×10^{14}	1.3×10^{14}	5×10^{14}	1×10^{14}	3×10^{13}
B	no	no	2×10^{15}	1×10^{14}	7×10^{14}	3×10^{14}	1×10^{13}
C	no	no	no	no	6×10^{14}	2×10^{14}	no
A1	3×10^{13}	7×10^{15}	5×10^{15}	no	1×10^{14}	no	no
B1	1×10^{15}	2×10^{15}	2×10^{15}	no	7×10^{13}	1×10^{13}	no
C1	7×10^{15}	yes	no	no	no	no	no

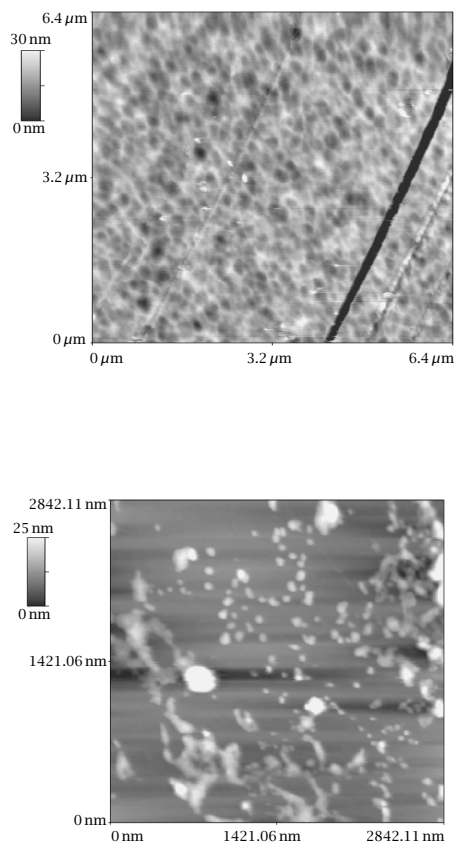


Figure 7. AFM images of the surfaces of a A and a B sample: the grayscale bar on the left represents the topographical height (coding black = 0, white = 30 nm for A and 25 nm for B).

The B samples have a structure clearly different from the A samples, with narrow and high hillocks surrounded by flat zones. A similar structure is observed by STM in Si wafers heated at high temperatures in high vacuum. An higher electrical activity of this type of structure with respect to the more homogeneous and bidimensional structure observed in the A samples can be the cause of the increase of the surface electrical activity observed in the B samples.

REFERENCES

- [1] D. K. Schröder, IEEE Trans. ED **44** (1997), 160.
- [2] B. W. Murray and H. R. Huff, J. Electrochem. Soc. **143** (1996), 1399.
- [3] S. M. Hu, C **139** (1991), 2066.
- [4] E. Susi, G. Lulli, and L. Passari, J. Electrochem. Soc. **134** (1987), 1239.
- [5] T. Y. Tan and C. Y. Kung, J. Appl. Phys. **59** (1986), 917.
- [6] H. Bender and J. Vanhellemont, Handbook on Semiconductors, **3** (1994), 1637.
- [7] K. Graff, Proc. Of the Satellite Symp. To ESSDERC '95, **3**, 1995.
- [8] M. Kittler and J. Lärz, Appl. Phys. Lett. **58** (1991), 911.
- [9] A. L. Rotondaro, T. Q. Hurd, et al., Proc. Of the Satellite Symp. To ESSDERC '95, **55**, 1995.
- [10] D. Walz, J. P. Joly, et al., Proc. Of the Satellite Symp. To ESSDERC '95, **64**, 1995.
- [11] M. Kittler, W. Seifert, and V. Higgs, MRS Symp. Proc. **378** (1995), 988.
- [12] P. Wagner, M. Brohl, et al., MRS Symp. Proc. **378** (1995), 17.
- [13] R. Brendel and M. Wolf, 13th Eur. Photov. Solar Energy Conf. Proc., **428**, 1995.
- [14] A. Poggi and E. Susi, J. Electrochem. Soc. **138** (1991), 1841.
- [15] A. Poggi and E. Susi, J. Electrochem. Soc. **141** (1994), 754.
- [16] E. Susi, A. Poggi, and M. Madrigali, J. Electrochem. Soc. **142** (1995), 2081.
- [17] S. J. Fonash, Solid State Technology **4** (1995), 201.
- [18] P. Pétri, P. Brault, et al., J. Appl. Phys. **75** (1994), 7498.
- [19] S. J. Fonash, J. Electrochem. Soc. **137** (1990), 3885.
- [20] M. Biavati, Q. I. Perez, et al., J. Vac. Sci. Techn. B **14** (1995), 2139.
- [21] G. Adegboyega, Q. I. Perez, et al., J. Vac. Sci. Techn. B **15** (1997), 623.
- [22] W. Gärtner, Phys. Rev. **105** (1957), 823.
- [23] J. Lagowski, A. M. Kontkiewicz, et al., **63** (1993), 2902.
- [24] H. B. DeVore, Phys. Rev. **102** (1956), 86.
- [25] P. Blood and J. W. Orton, *The Electrical Characterization of Semiconductors: Majority Carriers and Electron States*, p. 300, Academic Press, London, 1992.
- [26] A. Poggi, E. Susi, et al., J. Electrochem. Soc. **141** (1994), 754.
- [27] B. Mohadjeri, M. R. Baklanov, et al., J. Appl. Phys. **83** (1998), 3614.



Hindawi

Submit your manuscripts at
<http://www.hindawi.com>

